Single-cell analysis reveals the *KIT* D816V mutation in hematopoietic stem and progenitor cells in systemic mastocytosis

Brief title: Single-cell analysis in systemic mastocytosis

Jennine Grootens, MSc[a], Johanna S. Ungerstedt, MD, PhD[b,c], Maria Ekoff, PhD[a], Elin Rönnberg, PhD[a], Monika Klimkowska, MD, PhD[d], Rose-Marie Amini, MD, PhD[e], Michel Arock, PhD[f], Stina Söderlund, MD, PhD[g,h], Mattias Mattsson, MD[e,g], Gunnar Nilsson, PhD[a,g,h,*], and Joakim S. Dahlin, PhD[a,*]

Affiliations:

[a]Department of Medicine Solna, Karolinska Institutet, and Karolinska University Hospital, Stockholm, 17164, Sweden;

[b]Department of Medicine Huddinge, Karolinska Institutet, Stockholm, 14186, Sweden;

[c]Hematology Center, Karolinska University Hospital, Stockholm, 17176, Sweden;

[d]Department of Clinical Pathology and Cytology, Karolinska University Hospital Huddinge, Stockholm, 14186, Sweden;

[e]Department of Immunology, Genetics and Pathology, Uppsala University, Uppsala, 75185, Sweden;

[f]Molecular and Cellular Oncology, Ecole Normale Supérieure de Cachan, Cachan, 94235, France and Clinical Hematology Laboratory, Pitié-Salpêtrière Hospital, Paris, 75013, France;

[g]Division of Hematology, Uppsala University Hospital, Uppsala, 75185, Sweden;

[h]Department of Medical Sciences, Uppsala University, Uppsala, 75185, Sweden;

[*]Corresponding authors at: Department of Medicine, Division of Immuology and Allergy, Karolinska Institutet, 17164 Stockholm, Sweden.

Email addresses: gunnar.p.nilsson@ki.se (G.N. Nilsson), joakim.dahlin@ki.se (J.S. Dahlin).

Abstract

Background: Systemic mastocytosis (SM) is a hematological disease characterized by organ infiltration by neoplastic mast cells. Almost all SM patients have a mutation in the gene encoding the tyrosine kinase receptor KIT causing a D816V substitution and autoactivation of the receptor. Mast cells and $CD34^+$ hematopoietic progenitors can carry the mutation, however, in which progenitor cell subset the mutation arises is unknown. We aimed to investigate the distribution of the D816V mutation in single mast cells and single hematopoietic stem and progenitor cells.

Methods: Fluorescence-activated single-cell index sorting and D816V mutation assessment were applied to analyze mast cells and more than 10,000 $CD34^+$ bone marrow progenitors across 10 hematopoietic progenitor subsets. In vitro assays verified cell-forming potential.

Findings: We found that in SM 60-99% of the mast cells harbored the D816V mutation. Despite increased frequencies of mast cells in SM patients compared with control subjects, the hematopoietic progenitor subset frequencies were comparable. Nevertheless, the mutation could be detected throughout the hematopoietic landscape of SM patients, from hematopoietic stem cells to more lineage-primed progenitors. In addition, we demonstrate that $Fc\varepsilon RI^+$ bone marrow progenitors exhibit mast cell-forming potential, and we describe aberrant CD45RA expression on SM mast cells for the first time.

Interpretation: The *KIT* D816V mutation arises in early hematopoietic stem and progenitor cells and the mutation frequency is approaching 100% in mature mast cells, which express the aberrant marker CD45RA.

Key words (4-6)

Systemic Mastocytosis; Single-Cell; Mast Cell; Mast Cell Progenitor; CD45RA; Hematopoiesis; Hematopoietic Stem Cells; KIT D816V

Research in Context

Evidence before this study: Systemic mastocytosis is a myeloid neoplasm associated with a mutation in the receptor KIT. The mutation is found in multiple mature cell lineages and can be detected in bulk-sorted $CD34^+$ hematopoietic stem and progenitor cells.

Added value of this study: We use single-cell analysis to study the distribution of the common *KIT* mutation within the heterogenous $CD34^+$ progenitor landscape and in mast cells of systemic mastocytosis patients. Isolation of progenitor subsets followed by cell culture identifies a population of progenitors in bone marrow with increased mast cell-forming potential. Furthermore, a novel marker for aberrant mast cells in systemic mastocytosis is described.

Implications of all the available evidence: Our study provides novel insights into the cellular origin and propagation of the common *KIT* mutation in systemic mastocytosis. The identification of a novel marker for aberrant mast cells shows potential to improve disease diagnosis.

76 **Introduction**

77 Hematopoietic stem cells (HSCs) in the bone marrow give rise to blood cells and mast
78 cells. Differentiating HSCs progress through a number of intermediate progenitors
79 with multilineage-forming capacity before commitment to the mast cell lineage.[1,2]
80 The binding of stem cell factor (SCF) to its receptor, KIT, promotes the maturation
81 and proliferation of mast cells.[3-6] It is therefore not surprising that mutations in the
82 *KIT* gene coincide with the mast cell-driven disease systemic mastocytosis (SM).[7]
83

84 SM is a hematologic neoplasm in which infiltrates of neoplastic mast cells occur in
85 various tissues.[8,9] The majority of SM patients carry a mutation in *KIT*, most
86 commonly affecting codon 816.[10] The *KIT* D816V mutation makes receptor signaling
87 constitutively active, independent of binding to its ligand SCF. The detection of *KIT*
88 D816V in either bone marrow or peripheral blood samples is one of the criteria for the
89 clinical diagnosis of SM using a standardized qPCR assay.[11] When the *KIT* D816V
90 mutation is present in mast cells, it may also be detected in mature bone marrow or
91 peripheral blood cells, such as basophils, eosinophils, neutrophils, and B and T
92 lymphocytes, which depends on the patient.[12-17] Furthermore, the precursors of
93 erythroid and myeloid cells as well as $CD34^+$ progenitors may carry the *KIT* D816V
94 mutation.[12,18,19] Taken together, these findings suggest that the mutation may arise in
95 early hematopoietic stem and progenitor cells (HSPCs), rather than in a lineage-
96 restricted precursor.
97

98 The $CD34^+$ cell compartment is highly heterogeneous, spanning HSCs to late lineage-
99 committed progenitors. In the present study, we delineated the cellular origin of the
100 *KIT* D816V mutation in single bone marrow cells in SM by combining FACS index

101 sorting of $CD34^+$ HSPCs with a multiplex qPCR assay. The data revealed that the
102 D816V mutation in *KIT* arises in early HSPCs. The mutation burden is low but
103 variable in multipotent and lineage-restricted progenitor populations and increases in
104 mature mast cells. Furthermore, the present study provides more insight into
105 hematopoiesis in SM subjects and identifies high CD45RA expression in aberrant
106 mast cells.
107

108 **Materials and Methods**

109

110 *Patients and sample preparation*

111 Bone marrow and occasional peripheral blood samples were collected from patients
112 under evaluation for SM and from control subjects. The study was approved by the
113 Stockholm and Uppsala Regional Ethics committee. Oral and written informed
114 consent was obtained from each patient and control subject. The study was conducted
115 in accordance with the World Medical Association Declaration of Helsinki. The
116 patients included in our experimental studies were classified according to the World
117 Health Organization criteria[20] as having indolent SM (ISM, n = 19), aggressive SM
118 (ASM, n = 3), SM with associated hematological neoplasm (SM-AHN, n = 3), or
119 other malignancies, including myelodysplastic syndrome or myeloproliferative
120 neoplasm (MDS or MPN, n = 2). Supplementary Table 1 shows the patient
121 characteristics. For analytic purposes, ASM and SM-AHN patients were combined in
122 an advanced SM group (AdvSM). The controls (Ctrl) included patients with
123 cutaneous mastocytosis (CM, n = 2) and subjects without SM (n = 7). All samples
124 were processed on the day of collection. Red blood cells were lysed with PharmLyse
125 buffer (BD Biosciences, Franklin Lakes, NJ) and washed with PBS containing 2%
126 fetal calf serum (FCS, Thermo Fisher Scientific, Waltham, MA).

127

128 *Cell lines*

129 Two human mast cell lines, HMC-1.2 and ROSA$^{KIT\ WT}$, with and without the *KIT*
130 D816V mutation, respectively, were cultured as previously described.[21,22]

131

132 *Flow cytometry and cell sorting*

133 Bone marrow cells were stained with fluorophore-conjugated monoclonal antibodies
134 in Brilliant Stain Buffer (BD Biosciences, Franklin Lakes, NJ). The antibodies used
135 for staining included CD10 (HI10a), CD14 (M5E2), CD34 (581), CD38 (Hb7),
136 CD45RA (HI100), CD90 (5E10), CD117 (104D2), CD123 (6H6), CD133 (AC133),
137 and FcεRIα (CRA-1) (all from BD Biosciences, Biolegend, San Diego, CA, or
138 Miltenyi Biotec, Bergisch Gladbach, Germany). The live/dead cell marker DAPI (BD
139 Bioscience) was used for the analysis of cultured cells. Cell sorting and analysis were
140 performed using the FACSAria III and LSRFortessa systems (BD Biosciences). For
141 cell culture experiments, cells were sorted into sterile-filtered PBS with 2% FCS
142 following a two-step sorting protocol, using the yield followed by the purity precision
143 mode. The analysis of 20-100 sorted cells verified the sorting purity. Single $CD34^+$
144 cells were sorted into 2 µl of lysis buffer containing 20 µg/ml PCR-grade proteinase K
145 (Thermo Fisher Scientific) in EB buffer (Qiagen, Hilden, Germany). These cells were
146 sorted either immediately from the sample or following an enrichment sort. The
147 single-cell precision mode ensured that only one cell was deposited per well. The
148 plates were then centrifuged and stored at -80°C until analysis. The sorting data from
149 single cells were saved using the index sort module of the software FACSDIVA
150 software version 8 (BD Biosciences). Flow cytometry data analysis was performed
151 using FlowJo software version 10 (TreeStar, Ashland, OR).
152
153 *Cell culture and colony-forming assays*
154 Colony-forming potential was evaluated by plating 500 cells in 35 x 10 mm tissue
155 culture dishes (Thermo Fisher Scientific) in duplicate. The cells were cultured in
156 Methocult H4434, including SCF, IL-3, EPO, and GM-CSF (STEMCELL
157 Technologies Inc., Vancouver, Canada). Colonies were counted after 12-13 days,

158 distinguishing erythroid, granulocyte/monocyte, and mixed colonies following the
159 manufacturer's recommendations. The mast cell-forming potential was assessed via
160 liquid culture as described previously.[23] Briefly, sorted cells were cultured in medium
161 with recombinant human (rh) IL-3 (10 ng/mL; PeproTech, Rocky Hill, NJ) and rhIL-6
162 (10 ng/mL; PeproTech). In some experiments, the medium was changed on day 5, and
163 the cells were subsequently cultured with rhIL-6 (10 ng/mL) and SCF (100 ng/mL, r-
164 metHuSCF; Swedish Orphan Biovitrum, Stockholm, Sweden), as indicated in the
165 figure legends. Enzyme cytochemical staining of trypsin-like activity was used to
166 assess tryptase expression.[24,25] Cell morphology was evaluated by May-Grünwald
167 Giemsa staining (MGG; Sigma-Aldrich, St. Louis, MO).
168
169 *Single-cell mutation analysis*
170 Before the addition of lysis buffer, 96-well plates (Bio-Rad Laboratories, Hercules,
171 CA) were UV-treated for 30 minutes using a UVT-B-AR UV Cabinet (Grant
172 Instruments, Cambridge, UK). Tubes and pipettes were treated with the DNA AWAY
173 Surface Decontaminant (Thermo Fisher Scientific). After sorting, the cells were lysed
174 for 45 minutes at 55°C, followed by a 10-min heat-inactivating step at 95°C.
175 Multiplex qPCR analysis was performed via a Taqman gene expression assay
176 (Thermo Fisher Scientific) in lysed single cells using 96-well CFX Manager (Bio-Rad
177 Laboratories). A mutation assay was designed based on a previously published
178 method[11] using Primer3 (v.0.4.0) which specifically detected *KIT* c.2447A>T
179 (D816V) using the forward primer 5'-AGAGACTTGGCAGCCAGAAA-3'; a reverse
180 primer matching the mutation at the 3' position, 5'-
181 TTAACCACATAATTAGAATCATTCTTGATGA-3'; and the probe 5'-FAM-
182 TCCTCCTTACTCATGGTCGGATCACA-BHQ1-3'. A control assay was designed

183 to target a flanking exon and intron eight in GAPDH using the forward primer 5'-
184 CTGACTTCAACAGCGACACC-3'; the reverse primer 5'-
185 AGAGTTGTCAGGGCCCTTTT-3'; and the probe 5'-HEX-
186 TCAAGCTCATTTCCTGGTATGTG-BHQ1-3' (all primers came from TAG
187 Copenhagen, Denmark). The control and mutation assays were tested and optimized
188 using the cell lines ROSA$^{KIT\ WT}$ and HMC-1.2. The primer concentrations, optimized
189 for single cells, were as follows: control assay 150 nM forward/reverse primers, 100
190 nM probe; mutation assay 100 nM forward/reverse primers, 67 nM probe. Each plate,
191 containing 86 CD34^{+} cells, 5 mature mast cells, 3 empty wells, and 2 wells with bulk
192 CD34^{+} cells following sorting, was subjected to the multiplex qPCR assay. Cells were
193 excluded from analysis when amplification failed in the control assay, or when
194 amplification of the control assay resulted in a CT value higher than 40. In the
195 mutation assay, cells were regarded as unmutated when there was no amplification or
196 when the CT value was higher than 45. Outliers from each plate were then detected
197 using the ROUT outlier test in Prism software and removed from further analyses
198 (Supplementary Fig. 6B). Plates and cells that passed the quality control procedure
199 were linked with the index data and gated similarly to the whole sample for analysis.
200
201 *Statistical analysis*
202 Statistical analysis was performed using Prism software (Version 6.0h, GraphPad
203 Software, La Jolla, CA). The unpaired two-tailed Student's t-test was employed when
204 comparing two groups, and the unpaired one-way ANOVA with Tukey's multiple
205 comparison test was employed when comparing more than two groups. Statistical
206 analysis of log-transformed data was performed for some experiments as indicated in
207 the figure legends. Differences were considered significant when $P < 0.05$.
208

209 **Results**

210

211 *Systemic mastocytosis patients have a normal CD34^{+} bone marrow stem and*

212 *progenitor cell composition*

213 To assess the composition of the hematopoietic cells in the bone marrow of SM

214 patients, we designed a multicolor flow cytometry panel that identifies ten distinct

215 HSPC subtypes and mature mast cells (Table 1; Fig. 1A-B). Colony formation assays

216 confirmed the validity of the GMP, CMP, and MEP gating strategies in SM subjects

217 (Supplementary Fig. 1A-C). The flow cytometry data provided a specific HSPC

218 profile for 34 bone marrow samples: 9 control, 19 ISM and 6 AdvSM (Fig. 1C;

219 Supplementary Table 1). The percentages of HSPCs in SM samples did not

220 significantly differ from those in control samples (Fig. 1D and Supplementary Fig.

221 2A). In addition, the ISM and AdvSM samples exhibited percentages of total CD34^{+}

222 cells similar to the control samples (Supplementary Fig. 2B). Thus, the overall

223 hematopoiesis profile did not differ between the control and SM subjects.

224

225 *The bone marrow CMP$^{FcεRI+}$ fraction presents an enhanced mast cell-forming*

226 *potential*

227 Mast cell progenitors circulate in the blood as Lin^{-} CD34^{hi} CD117$^{int/hi}$ FcεRI^{+} cells.[33]

228 These cells express CD123 and lack CD45RA,[23,33] overlaying the CMP$^{FcεRI+}$ gate in

229 bone marrow (Supplementary Fig. 3A) that exhibit a distinct expression profile

230 compared with mature mast cells (Supplementary Fig. 3B). We therefore analyzed the

231 mast cell-forming potential of the bone marrow CMP$^{FcεRI+}$ fraction by culturing the

232 cells with IL-3 and IL-6. Flow cytometry analysis revealed that the CMP$^{FcεRI+}$ cultures

233 gave rise to a higher frequency of CD117^{hi} FcεRI^{+} mast cells than the CMPs$^{FcεRI-}$ cells

234 (Fig. 2A-C), despite overall lower CD117 expression (Supplementary Fig. 4A). May-
235 Grünwald Giemsa and enzymatic tryptase staining showed that the $CMP^{Fc\varepsilon RI+}$ progeny
236 generated a high frequency of granulated tryptase-positive mast cells when cultured
237 with SCF (Fig. 2D-E and Supplementary Fig. 5). Cultured GMPs did not give rise to
238 any cells with a mast cell phenotype (Fig. 2A-E and Supplementary Fig. 5).
239
240 The emerging model of hematopoiesis proposes that MEPs, basophils, and
241 eosinophils develop separately from GMPs following an asymmetric cell division at
242 the MPP stage. This process can be traced by the segregation of CD133, which is
243 expressed in GMPs but not in progenitors with erythromyeloid output.[34] Indeed, we
244 found that $CMP^{Fc\varepsilon RI+}$ cells exhibited only low levels of CD133 staining, similar to
245 erythromyeloid cells (Supplementary Fig. 4B).
246
247 *CD45RA is expressed on aberrant mast cells in systemic mastocytosis*
248 The multicolor flow cytometry panel used for the gating of HSPCs was also employed
249 to identify mast cells in bone marrow (Fig. 1B). May-Grünwald Giemsa and tryptase
250 staining confirmed that $CD14^{-}$ $CD34^{-}$ $CD117^{hi}$ $Fc\varepsilon RI^{hi}$ cells constitute mast cells (Fig.
251 3A). SM samples presented higher percentages of mast cells than controls (Fig. 3B).
252 Notably, mast cells from almost all SM samples exhibited aberrant CD45RA
253 expression, as verified with fluorescence minus one control and internal control
254 staining of $CD34^{+}$ cells (Fig. 3C-D). The cutaneous (non-systemic) mastocytosis
255 samples and MDS/MPN samples expressed low levels of CD45RA on bone marrow
256 mast cells (Fig. 3C-D). In addition, mast cell frequencies were correlated with the
257 clinical percentage of BMMC infiltrate and serum tryptase levels (Fig. 4A-C;
258 Supplementary Table 2). Taken together, the results indicate that SM bone marrow

259 samples contain more mast cells than control samples and these mast cells express
260 high levels of the aberrant marker CD45RA.
261
262 *Single-cell index sorting reveals the KIT D816V mutation in early HSPCs in systemic*
263 *mastocytosis patients*
264 The cellular origin of the *KIT* D816V mutation in SM has not been established, and
265 the relative abundance of this mutation in different $CD34^+$ HSPC populations and
266 mast cells has not been determined. We therefore developed a single-cell method to
267 trace the *KIT* D816V mutation using two cell lines: HMC-1.2 cells carrying the
268 mutation and ROSA cells carrying wild-type *KIT*. The cells were labeled with two
269 different fluorochrome-labeled antibodies, mixed, and randomly FACS sorted with
270 the index sort function. A multiplex qPCR assay was used to detect an irrelevant gene,
271 for quality control purposes, and the *KIT* D816V mutation (Supplementary Fig. 6A-
272 B). Among all single cells, more than 96% passed the quality control procedure
273 (Supplementary Fig. 6C). Linking the results with the index data revealed that the
274 mutation assay was negative for the wild-type ROSA cells. The assay detected the
275 mutation in 98.1% of all HMC-1.2 cells. Thus, the assay did not detect false positive
276 cells in the mutation assay and only a few false negatives, demonstrating the high
277 sensitivity and specificity of the method (Supplementary Fig. 6D).
278
279 The high success rate with cell lines allowed us to use the assay for HSPCs and
280 mature mast cells from patient samples. Single cells from 12 samples (6 ISM and 6
281 AdvSM) were analyzed for mutation assessment. Specifically, $CD34^+$ HSPCs were
282 index sorted from ten patients, whereas specific HSPC subsets were sorted from two
283 patients. At the time of SM diagnosis, the presence of the *KIT* D816V mutation was

284 confirmed in either peripheral blood or bone marrow (Supplementary Table 1). We
285 analyzed 40-194 single mast cells and 351-1583 single $CD34^+$ cells from each bone
286 marrow sample, providing mutation data for 12,859 single cells in total (Fig. 5A;
287 Supplementary Table 3). All SM samples carried the *KIT* D816V mutation in the mast
288 cell compartment at a high frequency in ISM (mean, 80.9%) and AdvSM (mean,
289 93.2%) (Fig. 5B). Index data analysis of individual mast cells demonstrated that
290 CD45RA expression was associated with presence of the *KIT* mutation (Fig. 5C). The
291 percentage of mutated mast cells was correlated with the total percentage of mast cells
292 in the sample and with the serum tryptase levels (Fig. 6A-B; Supplementary Table 2).
293 The mutation rate in $CD34^+$ HSPCs was less than 3% in all samples (Fig. 5D), except
294 for one AdvSM sample with a high mutation burden of 37.0% (Supplementary Table
295 4). Nevertheless, the percentage of mutated $CD34^+$ HSPCs was correlated with serum
296 tryptase levels (Fig. 6C; Supplementary Table 2).
297
298 Coupling the index data with the mutation analysis of 10 bone marrow samples
299 revealed that the *KIT* D816V mutation appeared throughout the hematopoietic
300 landscape (Fig. 5E; Supplementary Table 3-4). Specifically, different HSPCs
301 presented similar mutation rates in all samples when the median percentage of
302 mutation was compared between different HSPCs (Fig. 5F). Overall, the method of
303 index sorting provided a representative set of single cells from the whole-bone-
304 marrow aspirates (Supplementary Fig. 7A). However, the $CMP^{Fc\varepsilon RI+}$ population with
305 an enriched mast cell potential was rare. To determine the mutation frequency in the
306 $CMP^{Fc\varepsilon RI+}$ fraction, we selectively sorted 86 and 278 single $CMPs^{Fc\varepsilon RI+}$ from 2 SM
307 samples. One patient exhibited less than 2% mutated $CMPs^{Fc\varepsilon RI+}$, HSCs and GMPs,
308 whereas the fraction of mutated mast cells was 98.9% (Fig. 5G; Supplementary Table

309 4). The second patient presented 95.7% mutated CMPs$^{Fc\varepsilon RI+}$ and 96.4 % mutated mast

310 cells (Fig. 5H; Supplementary Table 4). Peripheral blood MCPs (CD14^{-} CD34^{+}

311 CD117^{+} FcεRI^{+}) showed mutation rates comparable to that of bone marrow

312 CMPs$^{Fc\varepsilon RI+}$ in one patient (Supplementary Fig. 7B), but the mutation could not be

313 detected in the MCPs from 4 other SM samples, likely due to the low mutation

314 frequency and the small number of cells analyzed due to the rarity of the cells (14-23

315 cells analyzed per sample). Taken together, we detected the *KIT* D816V mutation

316 throughout the hematopoietic landscape, starting with the HSCs.

317

318 **Discussion**

319

320 The cellular origin of the aberrant clone in SM is still under debate. Here, we show
321 that SM patients exhibit an increased frequency of mast cells in bone marrow. Almost
322 all these mast cells carry the *KIT* D816V mutation. Despite normal HSPC frequencies
323 in bone marrow, the *KIT* D816V mutation can be traced all the way back to the
324 $CD34^+$ $CD38^-$ $CD10^-$ $CD45RA^-$ $CD90^+$ HSC fraction.

325

326 The *KIT* D816V mutation causes receptor autoactivation, which signals survival,
327 proliferation, and differentiation, likely explaining the competitive growth advantage
328 of the aberrant mast cell clone and the high frequency of mutated mast cells.
329 However, the frequency of mutated HSPCs was low in most patients. This
330 observation is consistent with the overall normal HSPC composition of SM patients.
331 There are two main potential explanations for the low D816V mutation burden
332 observed in HSPCs relative to mast cells: HSPCs rapidly differentiate into mast cells
333 when the mutation occurs, or mutated HSPCs do not present a strong growth
334 advantage over non-mutated HSPCs. In fact, we have previously shown that KIT
335 signaling is dispensable for mast cell progenitor development in vitro and in vivo, and
336 that other stimuli can induce cell proliferation.[23] However, the aberrant progenitor
337 clone may in some cases proliferate to reach a high frequency, as demonstrated in two
338 patients with AdvSM who presented more than 20% mutated cells in the HSC
339 fraction. Advanced forms of SM have previously been associated with detection of
340 the *KIT* mutation in bulk-sorted $CD34^+$ progenitors and various mature cell lineages,
341 whereas in indolent disease, the mutation is mainly restricted to mast cells.[13]

342

343 It is of particular interest to study the mutation burden in progenitors with mast cell-
344 forming potential. We have previously reported that CD34^{+} CD117$^{int/hi}$ FcεRI^{+} cells in
345 peripheral blood are committed or nearly committed MCPs.[33] Considering the CD34^{+}
346 CD117^{+} FcεRI^{+} phenotype of CMPs$^{FcεRI+}$ cells, these cells might be expected to
347 present a similar mast cell-forming capacity as to blood MCPs. In the current study,
348 we showed that CMPs$^{FcεRI+}$ gave rise to a higher frequency of mast cells than
349 CMPs$^{FcεRI-}$ and GMPs. However, the mast cell frequency in cultured CMPs$^{FcεRI+}$ was
350 less than 10% and a substantial fraction were found to be CD117$^{-/lo}$ FcεRI^{+} cells after
351 culture, consistent with a basophil-like phenotype. Thus, CMPs$^{FcεRI+}$ exhibit a
352 considerable mast cell-forming capacity but also include progenitors with non-mast
353 cell output. Basophils mature in bone marrow, whereas mast cells mature in
354 peripheral tissues, which likely explains why bone marrow CMPs$^{FcεRI+}$ form CD117^{-}
355 FcεRI^{+} basophil-like cells, whereas CD34^{+} CD117$^{int/hi}$ FcεRI^{+} blood progenitors do
356 not. The high frequency of CD117^{-} FcεRI^{+} basophil-like cells that develop from
357 CMPs$^{FcεRI+}$ is also in agreement with the reduced CD117 expression of CMPs$^{FcεRI+}$
358 compared with that of CMPs$^{FcεRI-}$. CD117 is upregulated upon mast cell maturation,
359 and blood mast cell progenitors express intermediate to high levels of CD117.
360 CMPs$^{FcεRI+}$ express CD117 at low levels overall, even though there are individual
361 CMPs$^{FcεRI+}$ cells that express high CD117 levels, which might correspond to the cells
362 with mast cell-forming capacity. Taken together, our results indicate that the low *KIT*
363 mutation prevalence in the CMP$^{FcεRI+}$ fraction is likely explained by the capacity of
364 these cells' to form not only mast cells but also CD117^{-} FcεRI^{+} basophil-like cells.
365
366 In SM, mast cells are known to aberrantly express multiple surface proteins, among
367 CD2 and CD25 are currently used for diagnosis.[35] These markers are expressed

368 independently of the SM subtype. Other markers, such as CD30 and CD52, are
369 associated with AdvSM and mast cell leukemia.[36,37] In the present study, we
370 demonstrate that CD45RA is a novel marker for aberrant mast cells in SM.
371 Remarkably, bone marrow mast cells from two patients with cutaneous mastocytosis
372 expressed low CD45RA levels, suggesting that CD45RA is a marker for systemic
373 mast cell disease. The increase in the CD45RA isoform of CD45 likely explains the
374 high levels of CD45 observed in systemic mastocytosis patients.[38-41] Taken together,
375 our results indicate that high CD45RA expression should be considered a novel
376 marker for diagnosis of SM.
377
378 CD45RA is present on aberrant mast cells in SM, but at what stage during mast cell
379 differentiation is the marker upregulated? CMPs$^{FcεRI+}$, which lack CD45RA, present
380 mast cell-forming potential in SM patients. In contrast, we show that cells in the
381 classic CD45RA^{+} GMP gate lack mast cell potential in SM patients. An alternative
382 explanation is that the mast cell progenitors in SM fall into the immature CD38^{-} gate.
383 In fact, examples of rare mutated CD117$^{int/hi}$ FcεRI$^{int/hi}$ cells in the CD45RA^{+} LMPP
384 gate were seen (Supplementary Fig. 7C). It is also tempting to speculate that CD45RA
385 is upregulated once aberrant mast cells are mature.
386
387 The CD34^{+} HSPC population is highly heterogeneous and a single-cell resolution is
388 therefore necessary to delineate the cellular distribution of the mutation. Here, we
389 used single-cell index sorting to track cellular identity when performing mutation
390 analysis. Notably, the mutation was detected throughout differentiation, from HSCs to
391 the MEP, GMP, and LMPP fractions, depending on the patient. The detection of the

392 mutation in early HSPCs explains previous findings of the mutation being present in
393 bulk-sorted mature cell lineages of some patients.
394
395 Multiplex TaqMan qPCR assays detected the *KIT* mutation in index-sorted
396 progenitors in the present investigation. The qPCR method was originally developed
397 for sensitive mutation detection in DNA extracted from bone marrow or blood cells.
398 GAPDH primers and probes were added to the assay to confirm the presence or
399 absence of a sorted cell. This method allowed the detection of mutated cells with
400 close to 100% efficiency, with no observed false positives. The single-cell index
401 sorting and DNA mutation analysis approach can similarly be applied to other
402 mutations and hematologic diseases to reveal the origin of aberrant clones. One
403 limitation of the method is the number of cells that can be analyzed, meaning that
404 mutated cells in very rare subpopulations might go undetected. However, more than
405 10,000 HSPCs were analyzed in the present investigation, and single-cell index
406 sorting coupled with qPCR allowed unbiased and prospective analysis of mutated
407 HSPC populations in SM. Whole-genome amplification and nested PCR methods for
408 amplifying and sequencing DNA mutations from single cells are associated with the
409 phenomenon known as allelic dropout, which is the amplification of only a single
410 allele, leading to an overestimation of the frequency of non-mutated cells. Mutational
411 profiling of single colonies, as performed by Jawhar *et al.*[18] avoids this problem.
412 However, such analysis can be performed only on progenitors that form sufficiently
413 large colonies. Mast cell progenitors present a poor proliferative capacity, and this
414 technique was therefore not applied in the present investigation.
415

416 In summary, we have explored the composition and mutation profile of $CD34^+$ HSPCs
417 from SM patients. The results show that the *KIT* mutation can be found in cells
418 throughout the hematopoietic landscape with increased burden in the mast cell
419 lineage, supporting the notion that the aberrant clone may arise in the hematopoietic
420 stem cell compartment. Furthermore, the mutated mast cells express CD45RA, a
421 potential novel clinical biomarker for aberrant mast cells in SM.
422

423 **Acknowledgements**
424 We wish to thank Kerstin Hamberg Levedahl for help with the patients and Petter
425 Woll for helpful discussions. Stem cell factor was a kind gift from SOBI, Stockholm,
426 Sweden.
427

428 **Funding Sources**
429 This study was supported by the Swedish Research Council, the Swedish Cancer
430 Society, the Stockholm Cancer Society (Radiumhemmets Forskningsfonder), Magnus
431 Bergvall's Foundation, Tore Nilsson's Foundation for Medical Research, the
432 Karolinska Institutet, and through the regional agreement on medical training and
433 clinical research (ALF) between Stockholm County Council and the Karolinska
434 Institutet, and ALF-funding from Uppsala University Hospital.
435

436 **Declaration of Interest**
437 The authors declare no competing interests
438

439 **Author Contributions**

Conceptualization and Methodology, J.G., G.N. and J.S.D.; Investigation, J.G., M.E. and E.H.; Formal analysis, J.G.; Visualization and Validation, J.G. and J.S.D.; Resources, J.S.U., M.K., R.A., S.S., M.M. and M.A.; Writing – original draft, J.G. and J.S.D.; Writing – review & editing, all authors; Funding acquisition and Supervision, J.U., G.N. and J.S.D.

446 **References**

447 1. Dahlin JS, Hallgren J. Mast cell progenitors: origin, development and
448 migration to tissues. *Mol Immunol* 2015; **63**(1): 9-17.

449 2. Grootens J, Ungerstedt JS, Nilsson G, Dahlin JS. Deciphering the
450 differentiation trajectory from hematopoietic stem cells to mast cells. *Blood Adv* 2018;
451 **2**(17): 2273-81.

452 3. Irani AM, Nilsson G, Miettinen U, et al. Recombinant human stem cell factor
453 stimulates differentiation of mast cells from dispersed human fetal liver cells. *Blood*
454 1992; **80**(12): 3009-21.

455 4. Kirshenbaum AS, Goff JP, Kessler SW, Mican JM, Zsebo KM, Metcalfe DD.
456 Effect of IL-3 and stem cell factor on the appearance of human basophils and mast
457 cells from CD34+ pluripotent progenitor cells. *J Immunol* 1992; **148**(3): 772-7.

458 5. Valent P, Spanblochl E, Sperr WR, et al. Induction of differentiation of human
459 mast cells from bone marrow and peripheral blood mononuclear cells by recombinant
460 human stem cell factor/kit-ligand in long-term culture. *Blood* 1992; **80**(9): 2237-45.

461 6. Mitsui H, Furitsu T, Dvorak AM, et al. Development of human mast cells
462 from umbilical cord blood cells by recombinant human and murine c-kit ligand. *Proc*
463 *Natl Acad Sci U S A* 1993; **90**(2): 735-9.

464 7. Nagata H, Worobec AS, Oh CK, et al. Identification of a Point Mutation in the
465 Catalytic Domain of the Protooncogene C-Kit in Peripheral-Blood Mononuclear-Cells
466 of Patients Who Have Mastocytosis with an Associated Hematologic Disorder. *Proc*
467 *Natl Acad Sci U S A* 1995; **92**(23): 10560-4.

468 8. Valent P, Akin C, Escribano L, et al. Standards and standardization in
469 mastocytosis: consensus statements on diagnostics, treatment recommendations and
470 response criteria. *Eur J Clin Invest* 2007; **37**(6): 435-53.

471 9. Valent P, Akin C, Metcalfe DD. Mastocytosis: 2016 updated WHO
472 classification and novel emerging treatment concepts. *Blood* 2017; **129**(11): 1420-7.
473 10. Arock M, Sotlar K, Akin C, et al. KIT mutation analysis in mast cell
474 neoplasms: recommendations of the European Competence Network on Mastocytosis.
475 *Leukemia* 2015; **29**(6): 1223-32.
476 11. Kristensen T, Vestergaard H, Moller MB. Improved detection of the KIT
477 D816V mutation in patients with systemic mastocytosis using a quantitative and
478 highly sensitive real-time qPCR assay. *J Mol Diagn* 2011; **13**(2): 180-8.
479 12. Afonja O, Amorosi E, Ashman L, Takeshita K. Multilineage involvement and
480 erythropoietin-"independent" erythroid progenitor cells in a patient with systemic
481 mastocytosis. *Ann Hematol* 1998; **77**(4): 183-6.
482 13. Garcia-Montero AC, Jara-Acevedo M, Teodosio C, et al. KIT mutation in
483 mast cells and other bone marrow hematopoietic cell lineages in systemic mast cell
484 disorders: a prospective study of the Spanish Network on Mastocytosis (REMA) in a
485 series of 113 patients. *Blood* 2006; **108**(7): 2366-72.
486 14. Kocabas CN, Yavuz AS, Lipsky PE, Metcalfe DD, Akin C. Analysis of the
487 lineage relationship between mast cells and basophils using the c-kit D816V mutation
488 as a biologic signature. *J Allergy Clin Immunol* 2005; **115**(6): 1155-61.
489 15. Yavuz AS, Lipsky PE, Yavuz S, Metcalfe DD, Akin C. Evidence for the
490 involvement of a hematopoietic progenitor cell in systemic mastocytosis from single-
491 cell analysis of mutations in the c-kit gene. *Blood* 2002; **100**(2): 661-5.
492 16. Pardanani A, Reeder T, Li CY, Tefferi A. Eosinophils are derived from the
493 neoplastic clone in patients with systemic mastocytosis and eosinophilia. *Leuk Res*
494 2003; **27**(10): 883-5.

495 17. Mayado A, Teodosio C, Dasilva-Freire N, et al. Characterization of CD34(+)
496 hematopoietic cells in systemic mastocytosis: Potential role in disease dissemination.
497 *Allergy* 2018; **73**(6): 1294-304.
498 18. Jawhar M, Schwaab J, Schnittger S, et al. Molecular profiling of myeloid
499 progenitor cells in multi-mutated advanced systemic mastocytosis identifies KIT
500 D816V as a distinct and late event. *Leukemia* 2015; **29**(5): 1115-22.
501 19. Jara-Acevedo M, Teodosio C, Sanchez-Munoz L, et al. Detection of the KIT
502 D816V mutation in peripheral blood of systemic mastocytosis: diagnostic
503 implications. *Mod Pathol* 2015; **28**(8): 1138-49.
504 20. Arber DA, Orazi A, Hasserjian R, et al. The 2016 revision to the World Health
505 Organization classification of myeloid neoplasms and acute leukemia. *Blood* 2016;
506 **127**(20): 2391-405.
507 21. Saleh R, Wedeh G, Herrmann H, et al. A new human mast cell line expressing
508 a functional IgE receptor converts to tumorigenic growth by KIT D816V transfection.
509 *Blood* 2014; **124**(1): 111-20.
510 22. Sundstrom M, Vliagoftis H, Karlberg P, et al. Functional and phenotypic
511 studies of two variants of a human mast cell line with a distinct set of mutations in the
512 c-kit proto-oncogene. *Immunology* 2003; **108**(1): 89-97.
513 23. Dahlin JS, Ekoff M, Grootens J, et al. KIT signaling is dispensable for human
514 mast cell progenitor development. *Blood* 2017; **130**(16): 1785-94.
515 24. Harvima IT, Naukkarinen A, Harvima RJ, Fraki JE. Immunoperoxidase and
516 enzyme-histochemical demonstration of human skin tryptase in cutaneous mast cells
517 in normal and mastocytoma skin. *Arch Dermatol Res* 1988; **280**(6): 363-70.
518 25. Dahlin JS, Ungerstedt JS, Grootens J, et al. Detection of circulating mast cells
519 in advanced systemic mastocytosis. *Leukemia* 2016; **30**(9): 1953-6.

520 26. Notta F, Doulatov S, Laurenti E, Poeppl A, Jurisica I, Dick JE. Isolation of
521 Single Human Hematopoietic Stem Cells Capable of Long-Term Multilineage
522 Engraftment. *Science* 2011; **333**(6039): 218-21.
523 27. Majeti R, Park CY, Weissman IL. Identification of a hierarchy of multipotent
524 hematopoietic progenitors in human cord blood. *Cell Stem Cell* 2007; **1**(6): 635-45.
525 28. Manz MG, Miyamoto T, Akashi K, Weissman IL. Prospective isolation of
526 human clonogenic common myeloid progenitors. *Proc Natl Acad Sci U S A* 2002;
527 **99**(18): 11872-7.
528 29. Goardon N, Marchi E, Atzberger A, et al. Coexistence of LMPP-like and
529 GMP-like leukemia stem cells in acute myeloid leukemia. *Cancer Cell* 2011; **19**(1):
530 138-52.
531 30. Lee J, Breton G, Oliveira TY, et al. Restricted dendritic cell and monocyte
532 progenitors in human cord blood and bone marrow. *J Exp Med* 2015; **212**(3): 385-99.
533 31. Olweus J, BitMansour A, Warnke R, et al. Dendritic cell ontogeny: a human
534 dendritic cell lineage of myeloid origin. *Proc Natl Acad Sci U S A* 1997; **94**(23):
535 12551-6.
536 32. Doulatov S, Notta F, Eppert K, Nguyen LT, Ohashi PS, Dick JE. Revised map
537 of the human progenitor hierarchy shows the origin of macrophages and dendritic
538 cells in early lymphoid development. *Nat Immunol* 2010; **11**(7): 585-93.
539 33. Dahlin JS, Malinovschi A, Ohrvik H, et al. Lin- CD34hi CD117int/hi
540 FcepsilonRI+ cells in human blood constitute a rare population of mast cell
541 progenitors. *Blood* 2016; **127**(4): 383-91.
542 34. Gorgens A, Radtke S, Mollmann M, et al. Revision of the human
543 hematopoietic tree: granulocyte subtypes derive from distinct hematopoietic lineages.
544 *Cell Rep* 2013; **3**(5): 1539-52.

545 35. Teodosio C, Mayado A, Sanchez-Munoz L, et al. The immunophenotype of
546 mast cells and its utility in the diagnostic work-up of systemic mastocytosis. *J Leukoc*
547 *Biol* 2015; **97**(1): 49-59.
548 36. Sotlar K, Cerny-Reiterer S, Petat-Dutter K, et al. Aberrant expression of CD30
549 in neoplastic mast cells in high-grade mastocytosis. *Mod Pathol* 2011; **24**(4): 585-95.
550 37. Hoermann G, Blatt K, Greiner G, et al. CD52 is a molecular target in
551 advanced systemic mastocytosis. *FASEB J* 2014; **28**(8): 3540-51.
552 38. Chisholm KM, Merker JD, Gotlib JR, et al. Mast cells in systemic
553 mastocytosis have distinctly brighter CD45 expression by flow cytometry. *Am J Clin*
554 *Pathol* 2015; **143**(4): 527-34.
555 39. Escribano L, Diaz-Agustin B, Lopez A, et al. Immunophenotypic analysis of
556 mast cells in mastocytosis: When and how to do it. Proposals of the Spanish Network
557 on Mastocytosis (REMA). *Cytometry B Clin Cytom* 2004; **58**(1): 1-8.
558 40. Morgado JM, Sanchez-Munoz L, Teodosio CG, et al. Immunophenotyping in
559 systemic mastocytosis diagnosis: 'CD25 positive' alone is more informative than the
560 'CD25 and/or CD2' WHO criterion. *Mod Pathol* 2012; **25**(4): 516-21.
561 41. Teodosio C, Garcia-Montero AC, Jara-Acevedo M, et al. Mast cells from
562 different molecular and prognostic subtypes of systemic mastocytosis display distinct
563 immunophenotypes. *J Allergy Clin Immunol* 2010; **125**(3): 719-26, 26 e1-26 e4.
564

565 **Figure legends**

566

567 **Fig. 1**

568 **HSPC gating and profiling shows a normal course of hematopoiesis in patients**
569 **with systemic mastocytosis.** (A) A landscape model of the hematopoiesis. (B) Gating
570 strategy for bone marrow HSPCs and mature mast cells, showing representative plots
571 with population frequencies as percentages. (C) The hematopoietic progenitor profile
572 of 34 bone marrow samples. Cutaneous mastocytosis samples are indicated in italics.
573 (D) SM samples were compared with control samples without SM, including CM
574 (open circles), and the mean expression + SEM of each HSPC is presented as a
575 percentage of the total $CD34^{+}$ cells. The unpaired *t*-test was used in panel D to
576 compare the control and SM groups for each HSPC subset.

577

578 **Fig. 2**

579 **The $CMP^{Fc\varepsilon RI+}$ fraction in the bone marrow has mast cell potential.** (A-C) Flow
580 cytometry analysis of of $CMP^{Fc\varepsilon RI-}$, $CMP^{Fc\varepsilon RI+}$ and GMP cells cultured with rhIL-3
581 and rhIL-6 up to 21 days. (A) Flow cytometry plots of representative cultures,
582 showing the percentages of $CD117^{-}$, $CD117^{+}$, and $CD117^{hi}$ cells in each plot. (B)
583 Percentage of $CD117^{hi}$ $Fc\varepsilon RI^{+}$ cells at days 5-6. (C) Two of the samples in panel B
584 were followed for up to 21 days under culture with rhIL-3 and rhIL-6. The percentage
585 of $CD117^{hi}$ cells was analyzed on days 5-6, 13-14, and 19-21. (D) Representative
586 images of $CMP^{Fc\varepsilon RI-}$, $CMP^{Fc\varepsilon RI+}$ and GMP cells cultured with rhIL-3 and rhIL-6 for 5
587 days, followed by rhIL-6 and SCF until day 13-14, showing tryptase staining (red)
588 and granules by May-Grünwald Giemsa (MGG) staining. (E) Quantification of
589 tryptase-positive cells at days 13-14 and 17-21. $CMP^{Fc\varepsilon RI-}$, $CMP^{Fc\varepsilon RI+}$ cells were

590 analyzed from Ctrl29, SM28, SM32, SM33, and MDS30. GMPs were analyzed from
591 SM32 and SM33. The bars and lines in panel B, C and D represent the means ± SEM.
592 One-way ANOVA with Tukey's multiple comparison was used in panel B, $^{**}P <$
593 0.01, $^{***}P < 0.001$. Images were captured using an Olympus XC10 camera
594 (Olympus, Tokyo, Japan). The image width corresponds to 29 μm.
595
596 **Fig. 3**
597 **SM mast cells aberrantly express CD45RA.** (A) Enzymatic staining demonstrates
598 tryptase expression, and MGG staining reveals granules in SM mast cells. The images
599 are representative of two experiments (samples SM32 and SM33). Images were
600 captured using an Olympus XC10 camera (Olympus, Tokyo, Japan). The image width
601 corresponds to 29 μm. (B) Mast cell frequencies in Ctrl, ISM, AdvSM, and
602 MDS/MPN patients, showing the median of log-transformed values. (C) Histograms
603 showing CD45RA expression in mast cells (red line), FMO controls (grey histogram)
604 and $CD34^{+}$ cells (dotted line). (D) Frequency of CD45RA-expressing mast cells,
605 showing the mean and SEM. Control subjects included two subjects with CM (open
606 circles). One-way ANOVA with Tukey's multiple comparison was used in panels B
607 and D, $^{*}P < 0.05$, $^{**}P < 0.01$, $^{****}P < 0.0001$.
608
609 **Fig. 4**
610 **The percentage of mast cells in bone marrow correlates with clinical features.**
611 The percentage of mast cells was correlated with (A) serum tryptase levels and (B) the
612 percentage of BMMC infiltrate in the biopsy section. (C) Serum tryptase levels were
613 correlated with the percentage of BMMC infiltrate in the biopsy section. The samples
614 include ISM (closed dots) and AdvSM (open dots). Correlation values and

615 significance are indicated in the figure and in Supplementary Table 2. Linear
616 regression was calculated based on log-transformed data: in panel A, n = 25, and in
617 panels B and C, n = 23. The percentage of BMMC infiltrate was not determined for
618 two patients, accounting for the difference in numbers between panels. For analytical
619 purposes, BMMC infiltrate presented as <1% or <5% in Supplementary Table 1 were
620 set at 1% and 5% respectively.
621
622 **Fig. 5**
623 **Mutation analysis of KIT D816V in single cells identifies mutated HSPCs and**
624 **mast cells.** (A) Method of single-cell mutation analysis using index sorting and
625 multiplex qPCR. (B) The bars indicate the means + SEM percentage of mutated mast
626 cells. (C) The ratio between the median CD45RA expression of mutated and wild type
627 (WT) mast cells was determined for each patient. Each data point represents one
628 patient. The numbers of cells analyzed from each patient are presented in
629 Supplementary Table 3. Eleven patients are shown, as index data was not available
630 from 1 of the 12 patients. The two-tailed Wilcoxon signed rank test determined
631 whether the ratio was different from 1, indicated with a dotted line. $*P < 0.05$. (D)
632 The bars indicate the means + SEM percentage of mutated HSPCs. (E) The cellular
633 distribution of the mutation in 10 different HSPCs, showing the total numbers of
634 mutated and sorted cells for each sample that passed the quality control procedure. (F)
635 The bars indicate the median percentage of mutated cells per HSPC. (G-H) Mutation
636 frequencies of selectively isolated HSPCs following a 2-step sorting protocol in two
637 samples (SM28, ISM; and SM31, AdvSM). These two samples are indicated with
638 open circles in panels B and F.
639

640 **Fig. 6**

641 **The mutation rate in mast cells and HSPCs correlates with clinical features.**

642 (A-C) Linear regression of the percentage of mutated mast cells, showing significant

643 correlations with (A) the percentage of mast cells and (B) serum tryptase levels. (C)

644 The percentage of mutated HSPCs was correlated with serum tryptase levels. The

645 samples included ISM (closed dots) and AdvSM (open dots). Correlation and

646 significance are indicated in the figure and in Supplementary Table 2. Linear

647 regression was calculated based on log-transformed data in panels A-C, n = 12 and D,

648 n = 10.

649

650 **Table legend**

651 **Table 1. Immunophenotypes of HSPCs**

Fig. 1

A

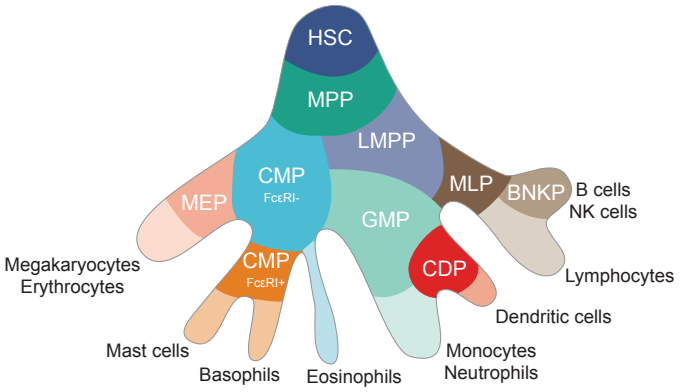
HSC
MPP
LMPP
CMP
FcεRI-
MEP
GMP
MLP
BNKP
B cells
NK cells
Megakaryocytes
Erythrocytes
CMP
FcεRI+
CDP
Lymphocytes
Dendritic cells
Mast cells
Basophils
Eosinophils
Monocytes
Neutrophils

B

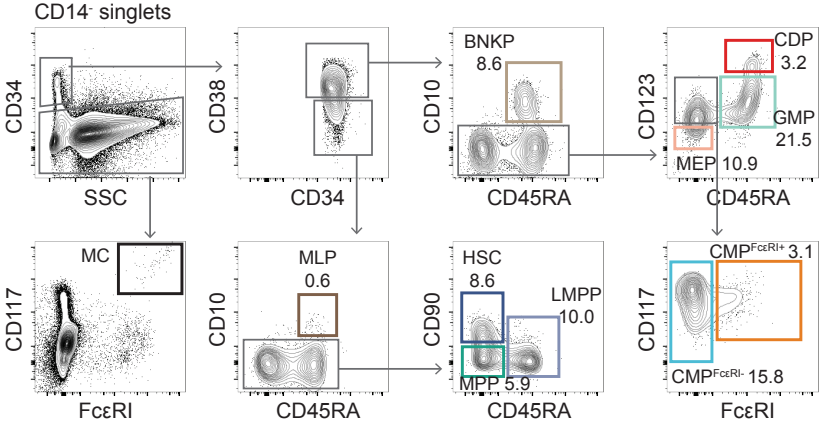
CD14- singlets
CD34
SSC
CD38
CD34
BNKP
8.6
CD10
CD45RA
CD123
CDP
3.2
GMP
21.5
MEP 10.9
CD45RA
MC
CD117
FcεRI
MLP
0.6
CD10
CD45RA
HSC
8.6
LMPP
10.0
MPP 5.9
CD90
CD45RA
CMPFcεRI+ 3.1
CD117
CMPFcεRI- 15.8
FcεRI

C

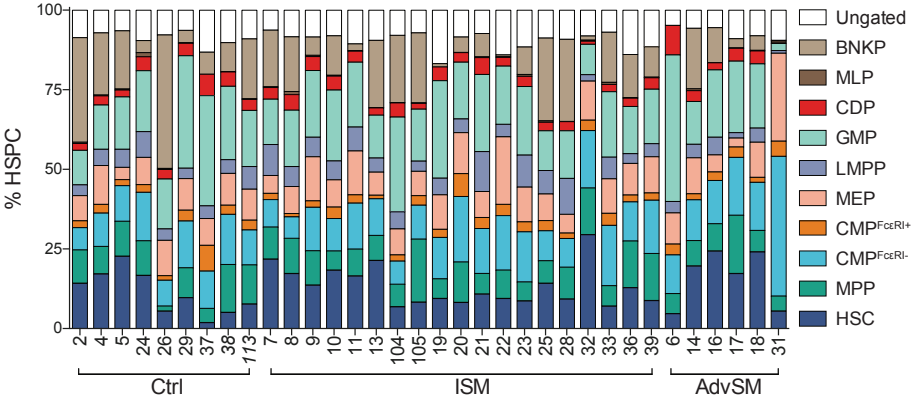
% HSPC
100
75
50
25
0
Ungated
BNKP
MLP
CDP
GMP
LMPP
MEP
CMPFcεRI+
CMPFcεRI-
MPP
HSC
2 4 5 24 26 29 37 38 113 7 8 9 10 11 13 104 105 19 20 21 22 23 25 28 32 33 36 39 6 14 16 17 18 31
Ctrl
ISM
AdvSM

D

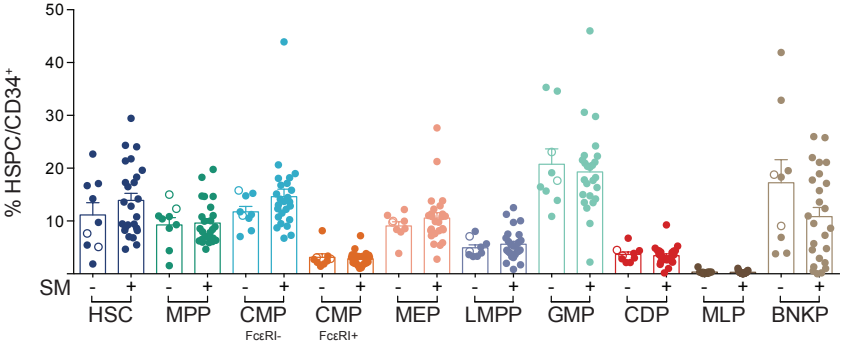
% HSPC/CD34+
50
40
30
20
10
SM
- +
HSC
MPP
CMP
FcεRI-
CMP
FcεRI+
MEP
LMPP
GMP
CDP
MLP
BNKP

Fig. 2

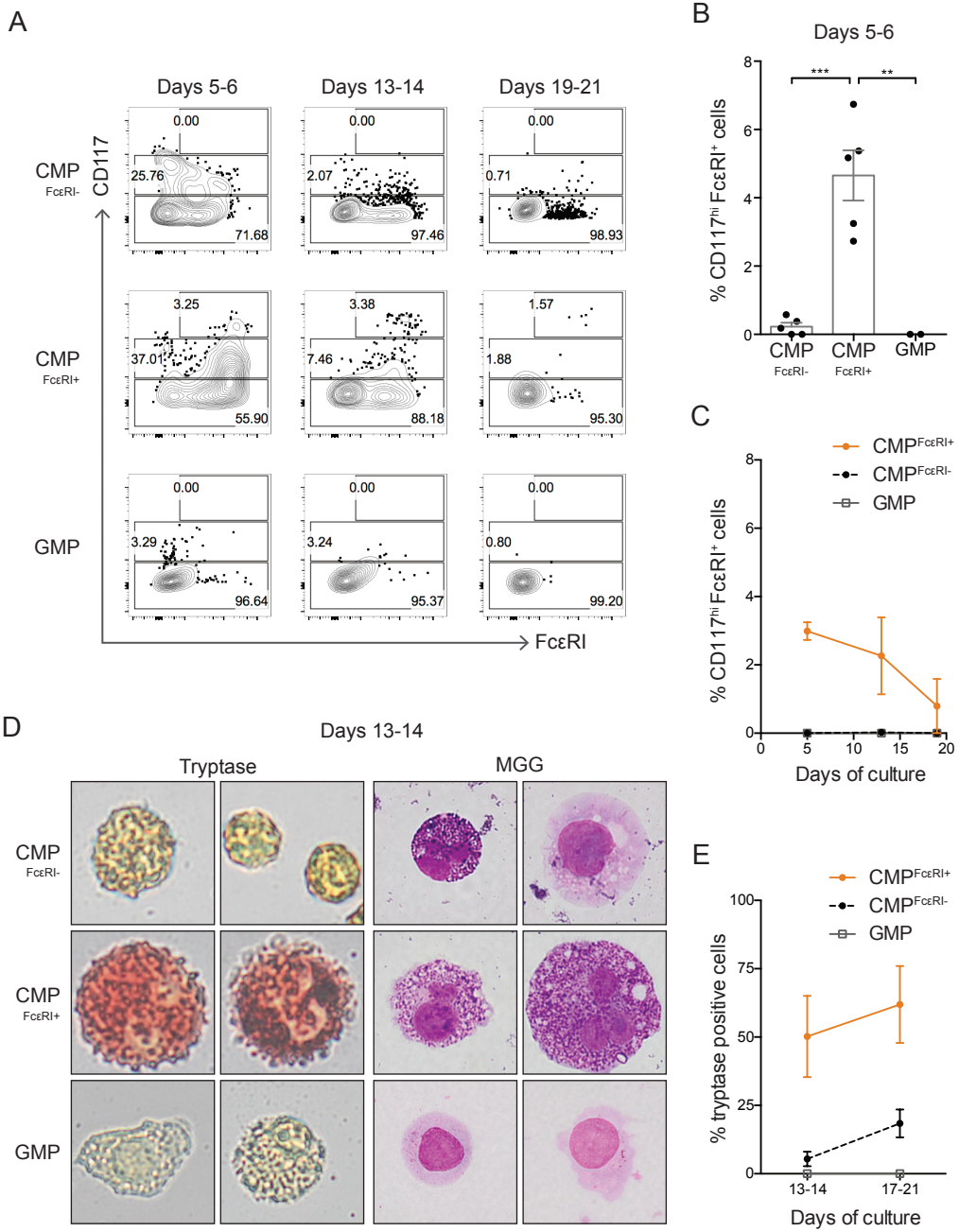
A
Days 5-6
Days 13-14
Days 19-21
CD117
CMP FcεRI-
CMP FcεRI+
GMP
FcεRI
0.00
25.76
71.68
0.00
2.07
97.46
0.00
0.71
98.93
3.25
37.01
55.90
3.38
7.46
88.18
1.57
1.88
95.30
0.00
3.29
96.64
0.00
3.24
95.37
0.00
0.80
99.20
B
Days 5-6
% CD117hi FcεRI+ cells
***
**
CMP FcεRI-
CMP FcεRI+
GMP
C
CMPFcεRI+
CMPFcεRI-
GMP
% CD117hi FcεRI+ cells
Days of culture
D
Days 13-14
Tryptase
MGG
CMP FcεRI-
CMP FcεRI+
GMP
E
CMPFcεRI+
CMPFcεRI-
GMP
% tryptase positive cells
13-14
17-21
Days of culture

Fig. 3

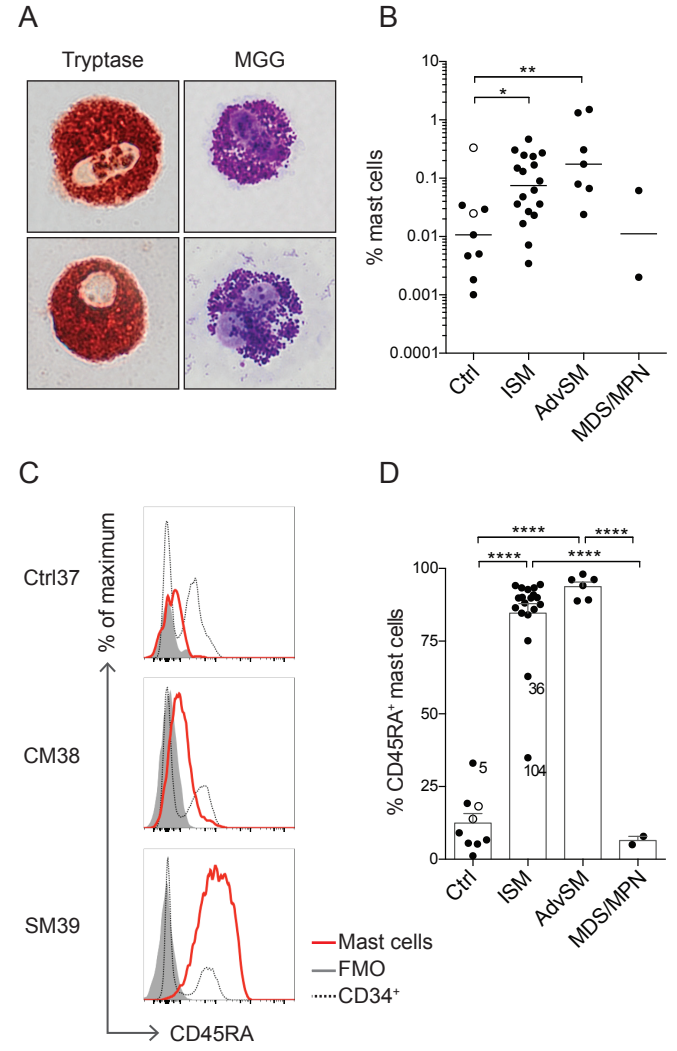
A
Tryptase
MGG
B
% mast cells
10
1
0.1
0.01
0.001
0.0001
**
*
Ctrl
ISM
AdvSM
MDS/MPN
C
% of maximum
Ctrl37
CM38
SM39
CD45RA
Mast cells
FMO
CD34+
D
% CD45RA+ mast cells
100
75
50
25
0
****
****
****
****
36
104
5
Ctrl
ISM
AdvSM
MDS/MPN

Fig. 4

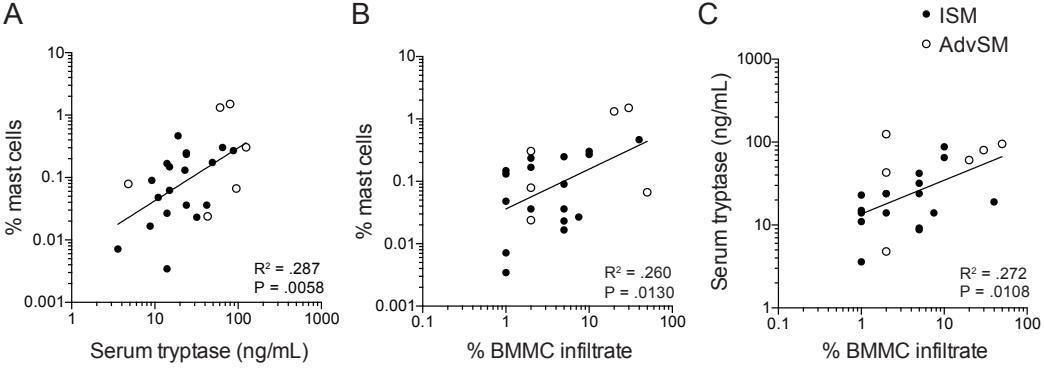
A
B
C
ISM
AdvSM
% mast cells
Serum tryptase (ng/mL)
R² = .287
P = .0058
% mast cells
% BMMC infiltrate
R² = .260
P = .0130
Serum tryptase (ng/mL)
% BMMC infiltrate
R² = .272
P = .0108

Fig. 5

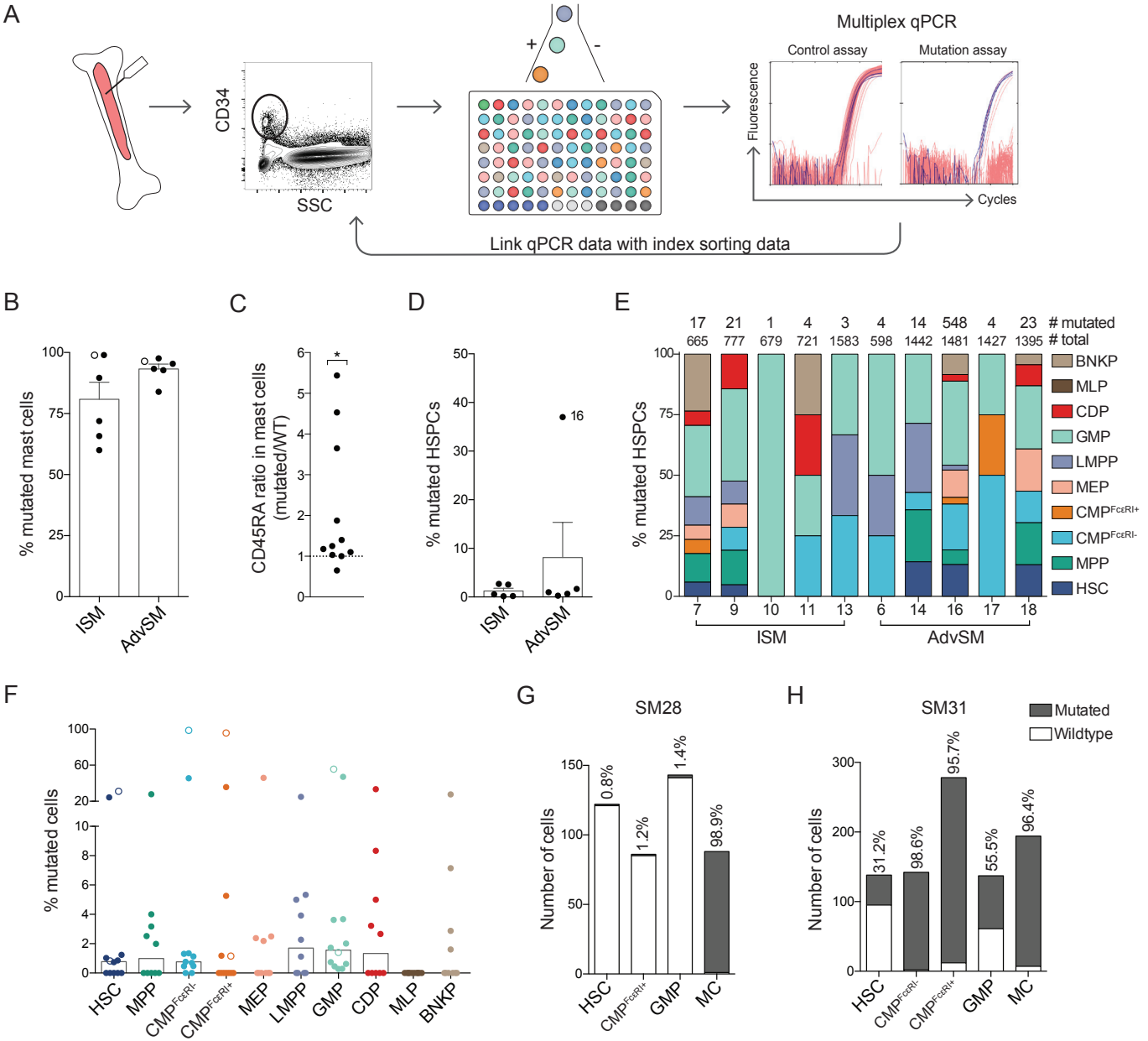
A
CD34
SSC
+
-
Multiplex qPCR
Control assay
Mutation assay
Fluorescence
Cycles
Link qPCR data with index sorting data
B
% mutated mast cells
ISM
AdvSM
C
CD45RA ratio in mast cells (mutated/WT)
*
D
% mutated HSPCs
16
ISM
AdvSM
E
mutated
total
17 21 1 4 3 4 14 548 4 23
665 777 679 721 1583 598 1442 1481 1427 1395
% mutated HSPCs
BNKP
MLP
CDP
GMP
LMPP
MEP
CMP^FcεRI+
CMP^FcεRI-
MPP
HSC
7 9 10 11 13 6 14 16 17 18
ISM
AdvSM
F
% mutated cells
HSC
MPP
CMP^FcεRI-
CMP^FcεRI+
MEP
LMPP
GMP
CDP
MLP
BNKP
G
SM28
Number of cells
0.8%
1.2%
1.4%
98.9%
HSC
CMP^FcεRI+
GMP
MC
H
SM31
Mutated
Wildtype
Number of cells
31.2%
98.6%
95.7%
55.5%
96.4%
HSC
CMP^FcεRI-
CMP^FcεRI+
GMP
MC

Fig. 6

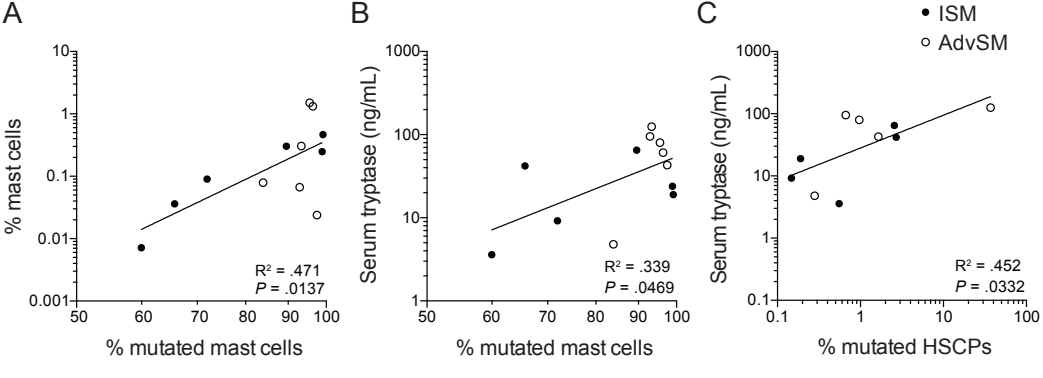
A
% mast cells
10
1
0.1
0.01
0.001
50
60
70
80
90
100
% mutated mast cells
R² = .471
P = .0137
B
Serum tryptase (ng/mL)
1000
100
10
1
50
60
70
80
90
100
% mutated mast cells
R² = .339
P = .0469
C
ISM
AdvSM
Serum tryptase (ng/mL)
1000
100
10
1
0.1
0.1
1
10
100
% mutated HSCPs
R² = .452
P = .0332

Table 1. Immunophenotypes of hematopoietic stem and progenitor cells

Short	Cell type	Gating strategy	References
HSC	Hematopoietic stem cell	$CD14^{-}$ $CD34^{+}$ $CD38^{-}$ $CD45RA^{-}$ $CD90^{+}$	26, 27
MPP	Multipotent progenitor	$CD14^{-}$ $CD34^{+}$ $CD38^{-}$ $CD45RA^{-}$ $CD90^{-}$	26, 27
$CMP^{FcεRI-}$	Common myeloid progenitor $FcεRI^{-}$	$CD14^{-}$ $CD34^{+}$ $CD38^{+}$ $CD45RA^{-}$ $CD10^{-}$ $CD123^{+}$ $FcεRI^{-}$	28 *
$CMP^{FcεRI+}$	Common myeloid progenitor $FcεRI^{+}$	$CD14^{-}$ $CD34^{+}$ $CD38^{+}$ $CD45RA^{-}$ $CD10^{-}$ $CD123^{+}$ $FcεRI^{+}$ $CD117^{+}$	28 *
MEP	Megakaryocyte-erythroid progenitor	$CD14^{-}$ $CD34^{+}$ $CD38^{+}$ $CD45RA^{-}$ $CD10^{-}$ $CD123^{-}$	28
LMPP	Lymphoid-primed multipotent progenitor	$CD14^{-}$ $CD34^{+}$ $CD38^{-}$ $CD45RA^{+}$	29
GMP	Granulocyte-monocyte progenitor	$CD14^{-}$ $CD34^{+}$ $CD38^{+}$ $CD45RA^{+}$ $CD10^{-}$ $CD123^{+}$	28
CDP	Common dendritic progenitor	$CD14^{-}$ $CD34^{+}$ $CD38^{+}$ $CD45RA^{+}$ $CD10^{-}$ $CD123^{hi}$	30, 31
MLP	Multilymphoid progenitor	$CD14^{-}$ $CD34^{+}$ $CD38^{-}$ $CD45RA^{+}$ $CD10^{+}$	32
BNKP	B- and NK cell progenitor	$CD14^{-}$ $CD34^{+}$ $CD38^{+}$ $CD45RA^{+}$ $CD10^{+}$	32
MC	Mast cell	$CD14^{-}$ $CD34^{-}$ $CD117^{hi}$ $FcεRI^{+}$	

*Refers to the original CMP population without the inclusion of the FcεRI marker.